SUPPLEMENTARY INFORMATION

Development of Machine-Learning Atomistic Potential for Molecular Simulation of Hematite-Water Interfaces

Mozhdeh Shiranirad and Niall J. English*[*]

School of Chemical and Bioproccess Engineering, University College Dublin, Belfield, D04 V1W8, Dublin, Ireland

E-mail: niall.english@ucd.ie

Symmetry function selection

The input vectors for the NNs were constructed using atom-centred symmetry functions (SFs).[1] For the Hematite-Water interface, not many studies using HNNP are available, so a careful selection of symmetry-functions was vital. Different methods have been proposed in the literature to generate input vectors with symmetry functions.[2–5]

Starting with the parameter set proposed in the literature,[5] we generated a set of 10 radial symmetry-functions (per pair) and four angular symmetry-functions per triples (with $\zeta \in \{1, 4\}$ and $\lambda = \pm 1$) using the Gastegger et.al. method[3] with a cutoff radius of 12 *Bohr*. This set of SFs were then screened in two stages

First, discarded the SFs whose range (i.e., maximum - minimum value over the entire data-set) were below 10^{-4}. Then, trained a model using this set of SFs and examined the prediction on an unseen test set; the RMSE of the predicted forces for the model was

2.5×10^{-1} $Hartree/Bohr$.

AS the second screen tried another set of SFs with 8 shifted radial SF (per pair) and 24 narrow angular SF per triple (with $\zeta \in \{1, 2, 4\}$ and $\lambda = \pm 1$); we again removed SFs with the range below 10^{-4}. The model from the second set gave us prediction with 57% RMSE improvement compare to the first set (from 2.5×10^{-1} to 1.06×10^{-1} $Hartree/Bohr$).
Secondly, performed a sensitivity analysis for trained models where the derivatives of the output neuron with respect to the input vector (i.e., symmetry-functions) were averaged over the whole data. This analysis removed the symmetry-functions with less than 0.5% sensitivity. Following this analysis, we could improve the RMSE of the initial set by 90% (from 1.06×10^{-1} to $2.41 \times 10^{-2} Hartree/Bohr$).
All symmetry-function values are scaled and centered based on the average and range of the individual symmetry-functions encountered in the training set according to

$$G_i = \frac{G_i - G_i^{avg}}{G_i^{max} - G_i^{min}}.$$

Model training

After selecting 20 random structures from the reference data pool, we computed their energy and forces using CP2K[6] through a single-energy calculation. The labeled data was then used to train a committee of eight HDNN models as the first generation. Each model was initialized with random weights and biases and trained separately. The training set for each model was created by random sub-sampling from the initial 20 structures, with 10% of the data points left out in each case to ensure the necessary diversity among committee members.[7]
To train the HDNN models, we utilized the open-source n2p2 code.[8] In each pool-based active-learning iteration, 20 new configurations are selected from a collection of candidate structures based on the highest committee disagreement in the atomic forces, as described

by Eq. 1 in the main text. Our calculations determined that the candidate set includes 10,000 structures from the structures pool. A new ensemble of models is then trained with the extended training set, which incorporates the newly chosen configurations.

After 13 iterations of active learning, convergence was achieved. Convergence was determined by observing a reduction in committee disagreement in subsequent iterations. Specifically, sampling stopped when there was no substantial difference in force disagreement between the "selected" points and those already in the "training" set. The convergence of disagreement for our case study is illustrated in Fig. S1. We tracked the evaluation of the atomic force disagreement for the structures in the "training," "selected," and "candidate" sets.

Init

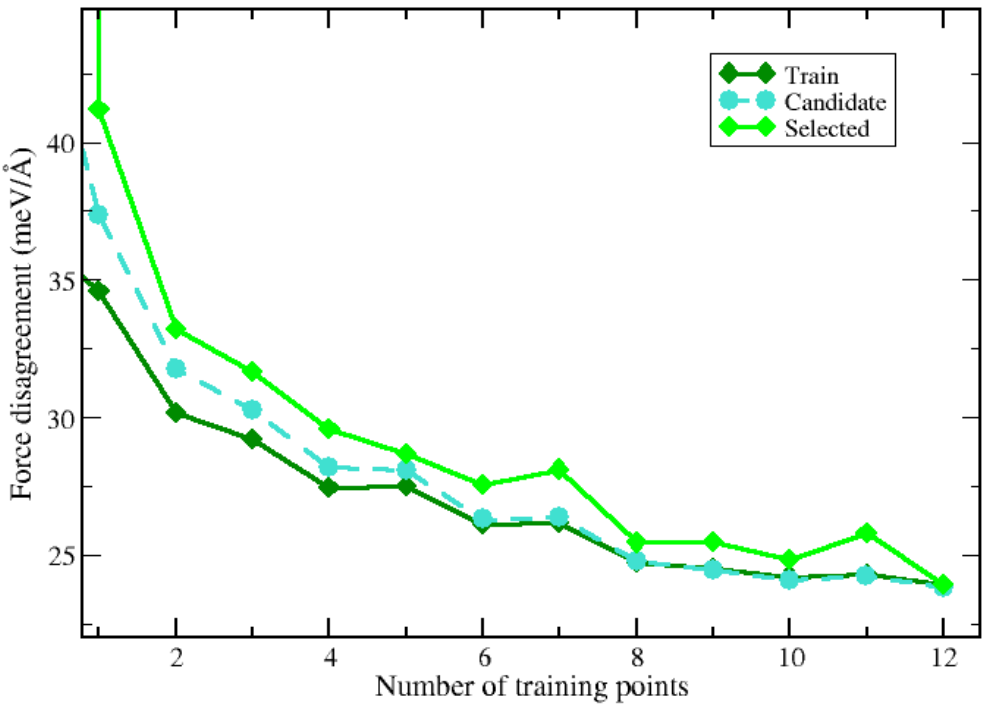


Figure S1: Convergence of the pool-based active-learning iterations with respect to the number of structures in the training set. The graph shows the mean-force committee disagreement for the training set (Train), the large set of potential new candidates (Candidates), and the actual newly-selected configurations (Selected).

the disagreement between the "selected" structures and those in the "training" and "candidate" sets is significant. However, as more points with the highest disagreement are added to the training set, this difference decreases monotonically. The committee force disagreement reported during active learning iterations can also be used to gauge the model's validity, as it represents an upper bound for accuracy.[7] This convergence indicates that a sufficient variety of structures has been sampled to yield an accurate and robust ensemble model. By this stage, our training set comprised approximately 300 structures.

After confirming there was no need for additional active-learning iterations, we performed a more robust training for all models in the committee to obtain the final ensemble model.

The NN models were constructed and trained using the n2p2 package.[8] Each model has two hidden layers with 20 neurons per layer, using the hyperbolic tangent activation function for the middle layer and a linear function for the last layer.

We used an adaptive global extended Kalman filter as the optimizer to adjust the network parameters.[8,9] Due to the time-consuming nature of training multiple networks (8 in our case), we trained the models loosely (15 epochs of multi-stream Kalman filter with 4 streams) during active-learning sampling, while the final model training was performed for 100 epochs using 32 streams. The ultimate model achieved the root mean squared error (RMSE) of the energy predictions of $\approx 0.96 \quad meV/atom$ and $\approx 447.16 \quad meV/\text{Å}$ for forces.

Model evaluation

The trained model was first evaluated against the reference force values for a smaller set of test data split from the labeled data. The comparison of predicted vs. reference values, shown in Figure S2, yielded a correlation of 0.98. To evaluate the model's performance, we utilized two properties: the radial distribution function (RDF) and power spectrum density (PSD). RDFs provide a comprehensive summary of the structural arrangement of a system, while PSDs illustrate its dynamical behavior.

We performed molecular dynamics simulations using the trained model for a system of the

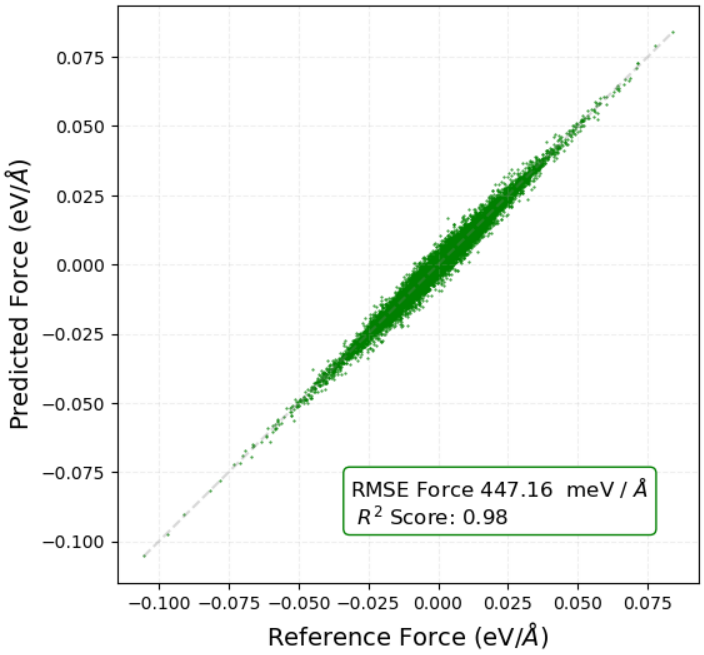


Figure S2: Predicted force compare to the reference values.

same size as the reference trajectory. The simulation was performed at 330 K and the time step of 0.5 fs. The duration of the simulation was 0.1 ns, which is twice that of the reference *ab-initio* trajectory. For this simulation, we used the CP2K software package.[6] The time for this simulation is about five hours, as opposed to about two and half months for the *ab-initio* MD computation for the reference data. We then compared the RDFs of the *ab-initio* reference trajectory to those predicted by the model based on the molecular dynamics simulation. Figure S3 presents a graphical representation of this comparison for oxygen atoms and also displays the total accuracy of the RDFs for all pairs in the system. Dynamical properties were validated by comparing the species-resolved power spectrum density (PSD) obtained from the model with that from the reference, providing a comprehensive overview of inter-molecular and intra-molecular motions. The distributions obtained using the AIMD and ensemble MD trajectories are plotted for all three elements in the system in Fig. S4. Although the distributions for the two trajectories are more in qualitative agreement in some regions, the peaks are in complete quantitative agreement, confirming the essential reliability of the model.

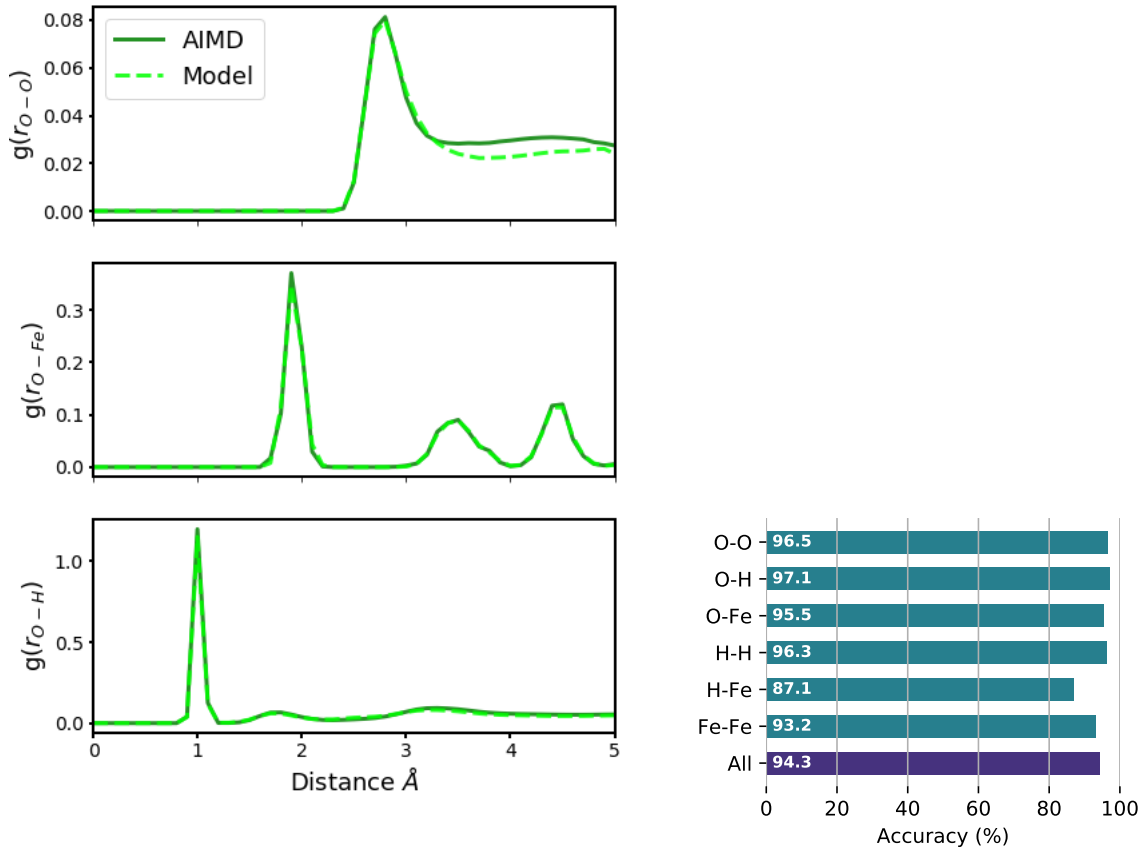


Figure S3: The RDFs correspond to atom Oxygen within both reference and cNNP model trajectories are plot. A summary of the accuracy of the model RDFs is represented (bottom); on average the cNNP model is 94.3% accurate in predicting RDFs.

References

(1) Behler, J.; Parrinello, M. Generalized neural-network representation of high-dimensional potential-energy surfaces. *Phys. Rev. Lett.* **2007**, *98*, 146401.

(2) Imbalzano, G., Anelli, A., Giofré, D., Klees, S., Behler, J. & Ceriotti, M. Automatic selection of atomic fingerprints and reference configurations for machine-learning potentials. *The Journal Of Chemical Physics.* **148**, 241730 (2018)

(3) Gastegger, M., Schwiedrzik, L., Bittermann, M., Berzsenyi, F. & Marquetand, P.

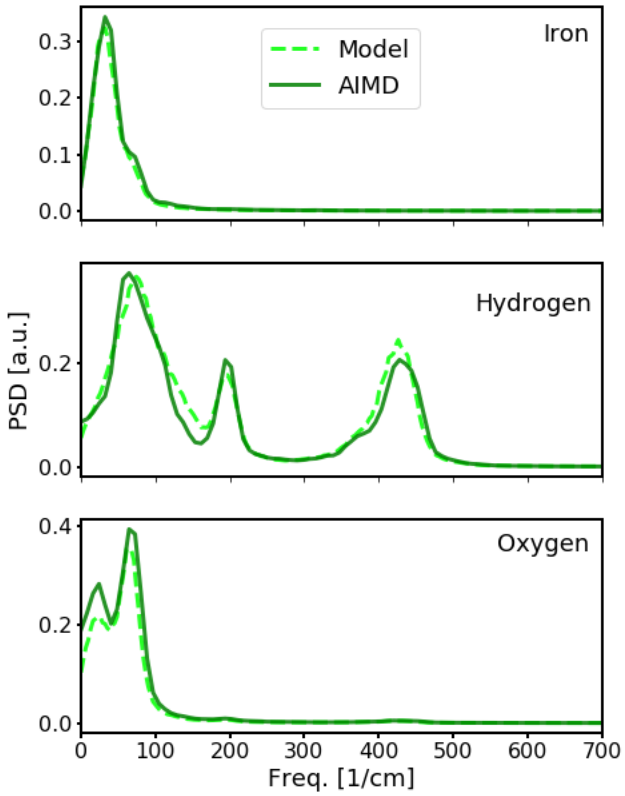


Figure S4: The PSD of all three components in the system are compared with the underlying AIMD trajectory.

wACSF—Weighted atom-centered symmetry functions as descriptors in machine learning potentials. *The Journal Of Chemical Physics*. **148**, 241709 (2018)

(4) Behler, J. Four Generations of High-Dimensional Neural Network Potentials. *Chem. Rev.* **2021**, *121*, 10037–10072.

(5) Schran, C.; Thiemann, F.; Rowe, P.; Müller, E.; Marsalek, O.; Michaelides, A. Machine learning potentials for complex aqueous systems made simple. *Proc. Natl. Acad. Sci. USA* **2021**, *118*, e2110077118.

(6) Kühne, T., Iannuzzi, M., Del Ben, M., Rybkin, V., Seewald, P., Stein, F., Laino, T., Khaliullin, R., Schütt, O., Schiffmann, F. & Others CP2K: An electronic structure

and molecular dynamics software package-Quickstep: Efficient and accurate electronic structure calculations. *The Journal Of Chemical Physics*. **152**, 194103 (2020)

(7) Schran, C.; Brezina, K.; Marsalek, O. Committee neural network potentials control generalization errors and enable active learning. *J. Chem. Phys.* **2020**, *153*, 104105.

(8) Singraber, A., Morawietz, T., Behler, J. & Dellago, C. Parallel multistream training of high-dimensional neural network potentials. *Journal Of Chemical Theory And Computation*. **15**, 3075-3092 (2019)

(9) Kalman, R. A new approach to linear filtering and prediction problems. *J. Basic Eng.* . **82**, 34-45 (1960)